Research Article

The Effect of Joint Damage on a Coal Wall and the Influence of Joints on the Abutment Pressure on a Fully Mechanised Working Face with Large Mining Height

Weibin Guo [ID], Shengwei Zhang [ID], and Yuhui Li [ID]

School of Energy Engineering, Key Laboratory of Western Mine Exploitation and Hazard Prevention with Ministry of Education, Xi'an University of Science and Technology, Xi'an, Shaanxi 710054, China

Correspondence should be addressed to Weibin Guo; guoweibin@xust.edu.cn

Coal wall spalling is regarded as a key technical problem influencing safe and efficient mining of large-mining-height working faces while the distribution of abutment pressure within the limit equilibrium zone (LEZ) influences coal wall spalling within a large-mining-height working face. This research attempted to explore the distribution characteristics of abutment pressure within the LEZ in a large-mining-height working face. For this purpose, the influences of the orientation of joints on mechanical characteristics of coal with joints and on the distribution of abutment pressure within the LEZ in the large-mining-height working face were analysed by theoretical analysis and numerical simulation. Research results show that the damage variable of coal with joints first rises, then decreases, and finally increases with increasing dip angle of the joints; as the azimuth of the joints increases, the damage variable first declines, then increases; the damage variable gradually declines with increasing joint spacing; an increase in the dip angle of joints corresponds to first reduction, then growth, and a final decrease of the abutment pressure at the same position in front of the coal walls; on certain conditions, the abutment pressure at the same position within the LEZ first rises, then declines as the azimuth of joints increases; with the growth of the joint spacing, the abutment pressure at the same position within the LEZ rises. The dip angle and azimuth of joints marginally affect the abutment pressure within the LEZ.

1. Introduction

Coal wall spalling is considered as a key technical problem influencing the safe, efficient, green, and intelligent mining of a fully mechanised working face with a large mining height (the mining height is bigger than 3.5 m), while the abutment pressure within the limit equilibrium zone (LEZ) during mining affects the stability of a coal wall [1–9]. There are many researches about the abutment pressure on the working face [10–15], which are mainly about the influences of roof structure, mining height, or the coal macroscopic mechanical parameters on the abutment pressure. The joint influence on the abutment pressure within the LEZ on the working face is almost rare. It is very important to analyse the joint influence to reveal the micro mechanism of the

abutment pressure distribution within the LEZ in the large-mining-height working face.

This paper attempted to find the relationship between the joint and the abutment pressure within the LEZ in the large-mining-height working face. Coal is formed slowly and numerous joints have developed under the complex geological conditions together with those induced by mining. From the perspective of damage mechanics, joints in coal account for the damage therein; therefore, it is possible to analyse the damage effect of joints on coal by establishing a constitutive equation for coal with joints. According to the limit equilibrium theory, the abutment pressure is mainly influenced by various factors (including support capacity of coal walls and mining height) within the LEZ in front of a large-mining-height working face [16]. In a large-mining-

height working face, the support capacity of coal walls can be calculated by using the theory on stability of columns [17–19]. Therefore, the support capacity of coal walls in a large-mining-height working face is mainly influenced by the dimensions of the coal walls and physico-mechanical parameters of the coal in the working face. Based on the limit equilibrium theory, the support capacity of coal walls in a large-mining-height working face is explored to reveal the distribution of abutment pressure within the LEZ in the large-mining-height working face based on joints and their displacement. It is of engineering significance to thus guarantee the stability of coal walls within the large-mining-height working faces.

The Brady Constitutive Equation for coal with joints was built firstly to analyse the influence of joints' parameters on damage in a coal wall, including the joints' dip angle, azimuth, and spacing. The relationships of the damage variable of coal containing through-going joints with the dip angle, azimuth, and spacing of joints are expressed by a formula. Then, based on the damage effect of joints on the coal, the abutment pressure within the LEZ in a large-mining-height working face was expressed by the formula containing the parameters of joints. Finally, the numerical simulation was used to verify the rationality of the formula of abutment pressure which reveal the distribution characteristics of abutment pressure within the LEZ influenced by the joints in a large-mining-height working face.

2. Influence of Joints on Damage in a Coal Wall

2.1. Brady Constitutive Equation for Coal with Joints.
Coal generally contains a group or multiple groups of joints with dominant orientation developed under long-term geological effects and mining-induced stress. Thus, it is feasible to simplify coal as rock containing a group or multiple groups of regularly distributed joints. On this basis, the influence of the orientation of joints on mechanical characteristics of coal can be attained according to the Brady model built by Olsson [20] and Brady et al. [21, 22].

Figure 1 shows the Brady mechanical model for coal with joints and the φ in Figure 1 means the internal frictional angle of the coal-rock blocks [21]. To simplify the analysis, the whole model for coal with joints is divided into two parts: joints with length L_g, in which only the part with the intermediate length of l_g is allowed to slide; coal-rock blocks in the upper and lower sides of joints.

The equivalent elastic stiffness of coal with joints can be deduced through analysis based on the Brady model [21]:

$$\frac{1}{k} = \frac{H}{WB_{\mathrm{b}}E} + \frac{\cos^2 \alpha}{K_n L_g B_{\mathrm{b}}} + \frac{\sin^2 \alpha}{K_s L_g B_{\mathrm{b}}}, \tag{1}$$

where

$$L_{\mathrm{g}} = \begin{cases} \dfrac{W}{\cos \alpha}, & \alpha \leq \arctan \dfrac{H}{W}, \\[4mm] \dfrac{H}{\sin \alpha}, & \alpha > \arctan \dfrac{H}{W}, \end{cases} \tag{2}$$

where k refers to the equivalent elastic stiffness of coal with a single joint; H, W, and B_b separately represent the height, width, and length of the model; E and a denote the elastic modulus of intact coal blocks and the dip angle of joints, respectively; K_n and K_s separately denote the normal and tangential stiffnesses of the joints.

2.2. The Influence of the Dip Angle of Joints.
Through analysis from the perspective of damage mechanics, the coal with joints can be considered as a damaged body. By introducing the damage variable D, the elastic modulus E_e for coal with joints is expressed as follows [23]:

$$E_e = (1 - D)E. \tag{3}$$

Under compression, the axial stiffness of coal with joints is calculated as follows [24]:

$$k = \frac{WB_b}{H}E_e. \tag{4}$$

Based on Equations (1) to (4), the damage variable D of coal with a single joint is expressed as follows:

$$D = \begin{cases} \dfrac{EK_n\sin^2 \alpha \cos \alpha + EK_s\cos^3 \alpha}{HK_nK_s + EK_n\sin^2 \alpha \cos \alpha + EK_s\cos^3 \alpha}, & \alpha \leq \arctan \dfrac{H}{W}, \\[5mm] \dfrac{EWK_n\sin^3 \alpha + EWK_s\cos^2 \alpha \sin \alpha}{H^2K_nK_s + EWK_n\sin^3 \alpha + EWK_s\cos^2 \alpha \sin \alpha}, & \alpha > \arctan \dfrac{H}{W}. \end{cases} \tag{5}$$

As shown in Equation (5), the equivalent elastic modulus of coal with joints is related to the elastic modulus of coal blocks, the dip angle, normal stiffness, and tangential stiffness of joints as well as the height of coal-rock blocks containing the joints. When $E = 10$ GPa, $K_n = 10$ GPa/m, $K_s = 4$ GPa/m [25], and $H = 2W = 2$ m [21], the change in the damage variable of coal with a single joint with the dip angle of the joint is displayed in Figure 2.

It can be seen from Figure 2 that an increase of the dip angle of the joint corresponds to initial growth, then a decrease, and a final increase of the damage variable of coal with a single joint; the damage variable varies between 0.33
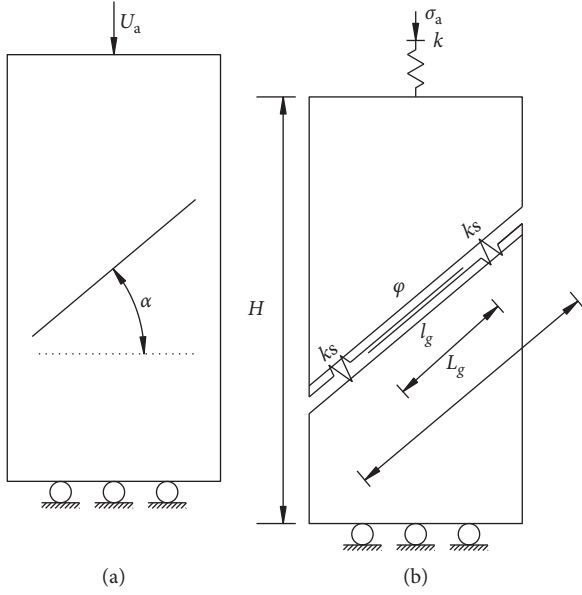
(a) (b)

FIGURE 1: Brady model of coal body containing joints. (a) Coal with a single joint. (b) Equivalent physical model.

and 0.39: the change in the dip angle of the joint influences the damage, albeit to an insignificant extent.

2.3. The Influence of the Azimuth of the Joints.

In the Brady model, the length L_g of joints certainly varies when their dip angle satisfies $\alpha \leq \arctan(H/W)$ under the influence of β, the azimuth of joints. The relationship of L_g to α and β is attained:

$$L_g = \begin{cases} \dfrac{B_b}{\cos\alpha\cos\beta}, & \beta \leq \arctan\dfrac{W}{B_b}, \\[3mm] \dfrac{W}{\cos\alpha\sin\beta}, & \beta > \arctan\dfrac{W}{B_b}. \end{cases} \quad (6)$$

The length of joints satisfies Equation (2) when their dip angle satisfies $\alpha > \arctan(H/W)$. According to Equation (1),
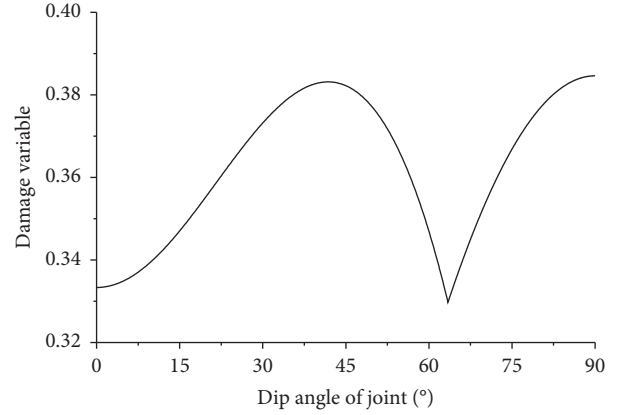

FIGURE 2: The change in the damage variable of coal body containing a joint with inclination angle of the joint.

the equivalent elastic stiffness of coal with a single joint at different azimuths still can be calculated. It is only necessary to replace L_g in the equation with Equation (2) or Equation (6) according to different conditions. The rationality of the above analysis can be validated by employing 3DEC numerical simulation, as shown in Figure 3. The parameters used in the numerical simulation are equal to the parameters used in the theoretical analysis. It can be seen from the figure that the curves obtained through numerical simulation are consistent with those attained through theoretical analysis under different dip angles and azimuths of joints, which reveals the rationality of the above theoretical analysis.

It can be found from the above analysis that at different azimuths of joints, the damage variable D of coal with a single joint is unaffected by the azimuth while being associated only with the dip angle of the joint when the dip angle satisfies $\alpha > \arctan(H/W)$. In this case, the expression of the damage variable is the same as that in Equation (5); at $\alpha \leq \arctan(H/W)$, the damage variable D of coal with a single joint is expressed in Equation (7) due to changes in azimuth and the dip angle:

$$D = \begin{cases} \dfrac{EWK_n\sin^2\alpha\cos\alpha\cos\beta + EWK_s\cos^3\alpha\cos\beta}{B_bHK_nK_s + EWK_n\sin^2\alpha\cos\alpha\cos\beta + EWK_s\cos^3\alpha\cos\beta}, & \beta \leq \arctan\dfrac{W}{B_b}, \\[4mm] \dfrac{EK_n\sin^2\alpha\cos\alpha\sin\beta + EK_s\cos^3\alpha\sin\beta}{HK_nK_s + EK_n\sin^2\alpha\cos\alpha\sin\beta + EK_s\cos^3\alpha\sin\beta}, & \beta > \arctan\dfrac{W}{B_b}. \end{cases} \quad (7)$$

According to Equation (7), the change in the damage variable of coal with joint with the azimuth under different dip angles of the joint is attained given $E = 10\,\text{GPa}$, $K_n = 10\,\text{GPa/m}$, $K_s = 4\,\text{GPa/m}$, and $H = 2B_b = 2W = 2\,\text{m}$, as shown in Figure 4.

As shown in Figure 4, the damage variables of coal with a single joint first decrease, then increase under the influence

of the azimuth at different dip angles of the joint; however, the difference varies; at $B = W$, the azimuth $\beta = 45°$ is taken as the dividing point in Equation (7) and therefore the damage variables are all minimised in this condition. At the dip angle of the joint of 30°, the damage variable varies from 0.30 to 0.37; the damage variable varies between 0.30 and 0.38 at the dip angle of 60°; at the dip angle of 45°, the damage variable
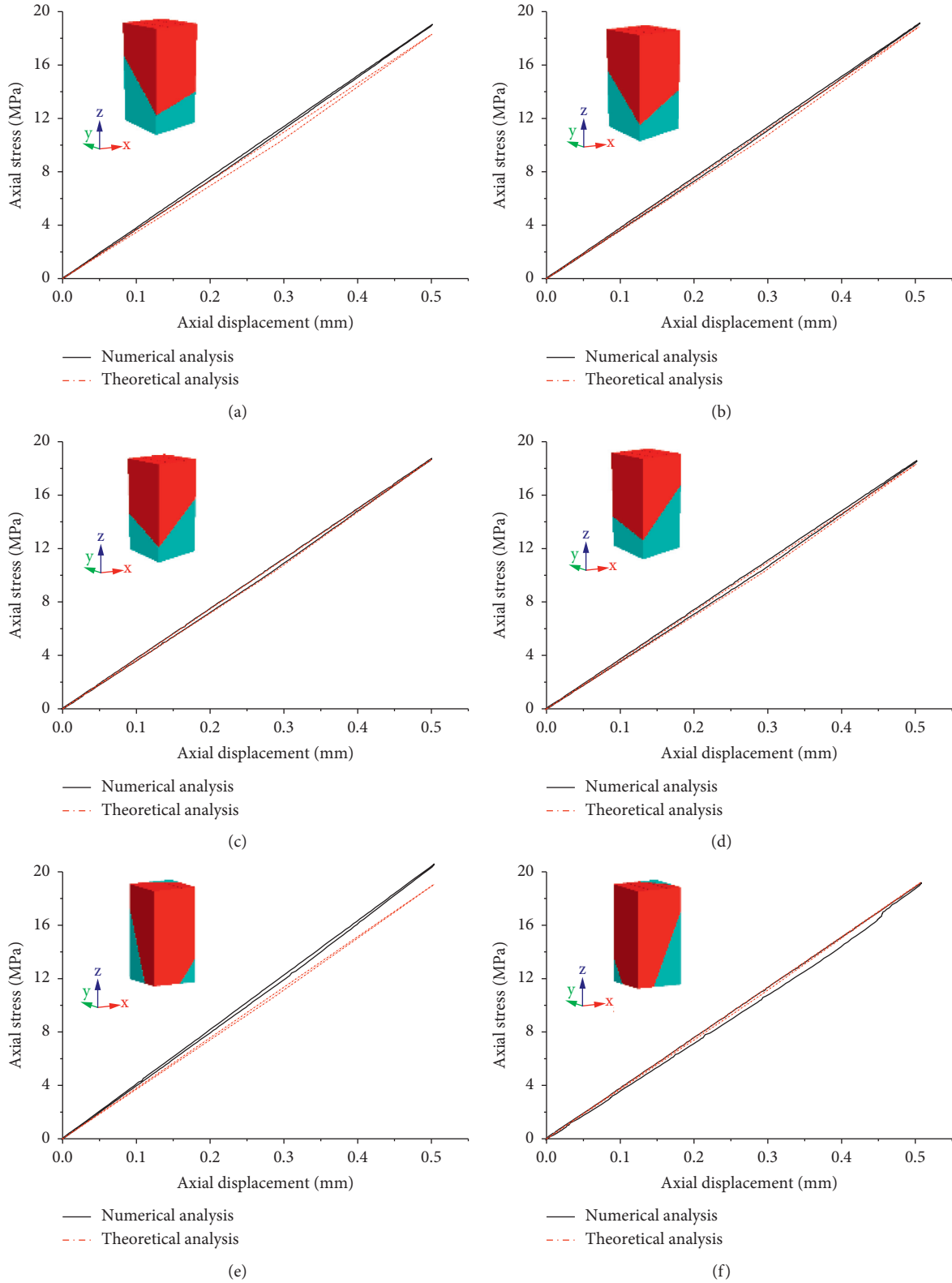
FIGURE 3: Comparison of numerical and theoretical results at different azimuth angles (a) $\alpha = 45°$ and $\beta = 15°$. (b) $\alpha = 45°$ and $\beta = 30°$. (c) $\alpha = 45°$ and $\beta = 60°$. (d) $\alpha = 45°$ and $\beta = 75°$. (e) $\alpha = 70°$ and $\beta = 30°$. (f) $\alpha = 70°$ and $\beta = 60°$.

varies between 0.27 and 0.35. As a result, the change of the azimuth of a joint affects the coal with the joint (albeit to an insignificant extent).

2.4. The Influence of the Joint Spacing. Apart from the dip angle α and azimuth β, the spacing d is also considered an important parameter for joints. According to the
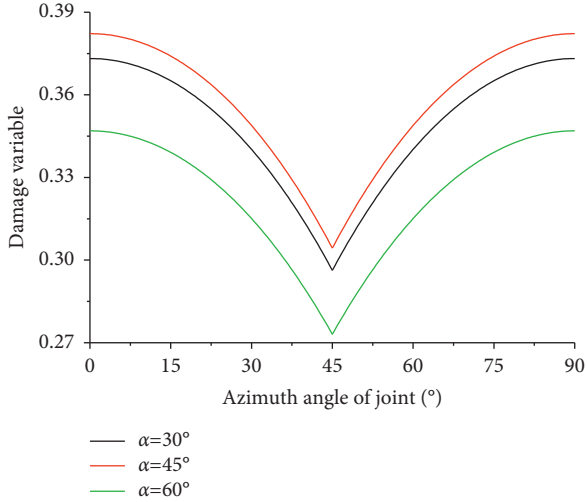
FIGURE 4: The change in the damage variable of a coal body containing a joint with azimuth angle of the joint.

superposition principle, the Brady model can be extended to complex situations containing two or multiple parallel joints. In this way, the influence of the joint spacing on the damage variable of coal with joints is ascertained. The complex situation containing two or multiple parallel joints can be considered as comprising two (or more) simple Brady mechanical models and one or more models for intact coal-rock blocks. By taking a model for coal with two joints as an example, the model for coal can be equivalent to two simple Brady models for coal with joints and a model for intact coal-

rock blocks (Figure 5) to analyse the damage modulus of coal containing joints.

The global displacement of coal with two joints is calculated as follows:

$$U_a = U_b + U_c - U_0, \tag{8}$$

where U_b, U_c, and U_0 separately refer to displacements of various component elements. The equivalent elastic stiffness of coal containing two joints is expressed as follows:

$$\frac{1}{k_2} = \frac{H}{WB_bE} + \frac{2\cos^2 \alpha}{K_nL_gB_b} + \frac{2\sin^2 \alpha}{K_sL_gB_b}, \tag{9}$$

where the meanings of various physico-mechanical parameters follow those in Equations (1) and (2).

By taking $H = 2W = 2$ m and $\alpha = 45°$ as an example, the curves attained through 3DEC numerical simulation software highly coincide with those obtained through theoretical analysis (Figure 6), which indicates the rationality of the above theoretical analysis.

In the Brady model, it is supposed that the normal stress on joints is uniformly distributed and joints are elastically extended; stress concentration (especially, normal stress concentration on joints) occurs during numerical simulation. Therefore, the curves attained through numerical simulation are not completely in line with those obtained through theoretical analysis (Figures 3 and 6).

According to the above analysis, the damage variable D_2 of two coal containing joints is calculated as follows:

$$D_2 = \begin{cases} \dfrac{2EK_n\sin^2 \alpha \cos \alpha + 2EK_s\cos^3 \alpha}{HK_nK_s + 2EK_n\sin^2 \alpha \cos \alpha + 2EK_s\cos^3 \alpha}, & \alpha \leq \arctan\dfrac{H}{W}, \\[4mm] \dfrac{2EWK_n\sin^3 \alpha + 2EWK_s\cos^2 \alpha \sin \alpha}{H^2K_nK_s + 2EWK_n\sin^3 \alpha + 2EWK_s\cos^2 \alpha \sin \alpha}, & \alpha > \arctan\dfrac{H}{W}. \end{cases} \tag{10}$$

Similarly, when n (a positive integer) through-going joints are found in coal, the damage variable D_n is calculated as follows:

$$D_n = \begin{cases} \dfrac{nEK_n\sin^2 \alpha \cos \alpha + nEK_s\cos^3 \alpha}{HK_nK_s + nEK_n\sin^2 \alpha \cos \alpha + nEK_s\cos^3 \alpha}, & \alpha \leq \arctan\dfrac{H}{W}, \\[4mm] \dfrac{nEWK_n\sin^3 \alpha + nEWK_s\cos^2 \alpha \sin \alpha}{H^2K_nK_s + nEWK_n\sin^3 \alpha + nEWK_s\cos^2 \alpha \sin \alpha}, & \alpha > \arctan\dfrac{H}{W}. \end{cases} \tag{11}$$

According to Equation (11), the change in the damage variable of coal with the number of joints therein at different dip angles when $E = 10$ GPa, $K_n = 10$ GPa/m, $K_s = 4$ GPa/m, and $H = 2W = 2$ m can be attained (Figure 7 and Table 1).

The change curves of the damage variable at different dip angles of joints basically coincide, which indicates consistent changes to the damage variable with the number of joints; with the growth of the number of joints, the damage variable
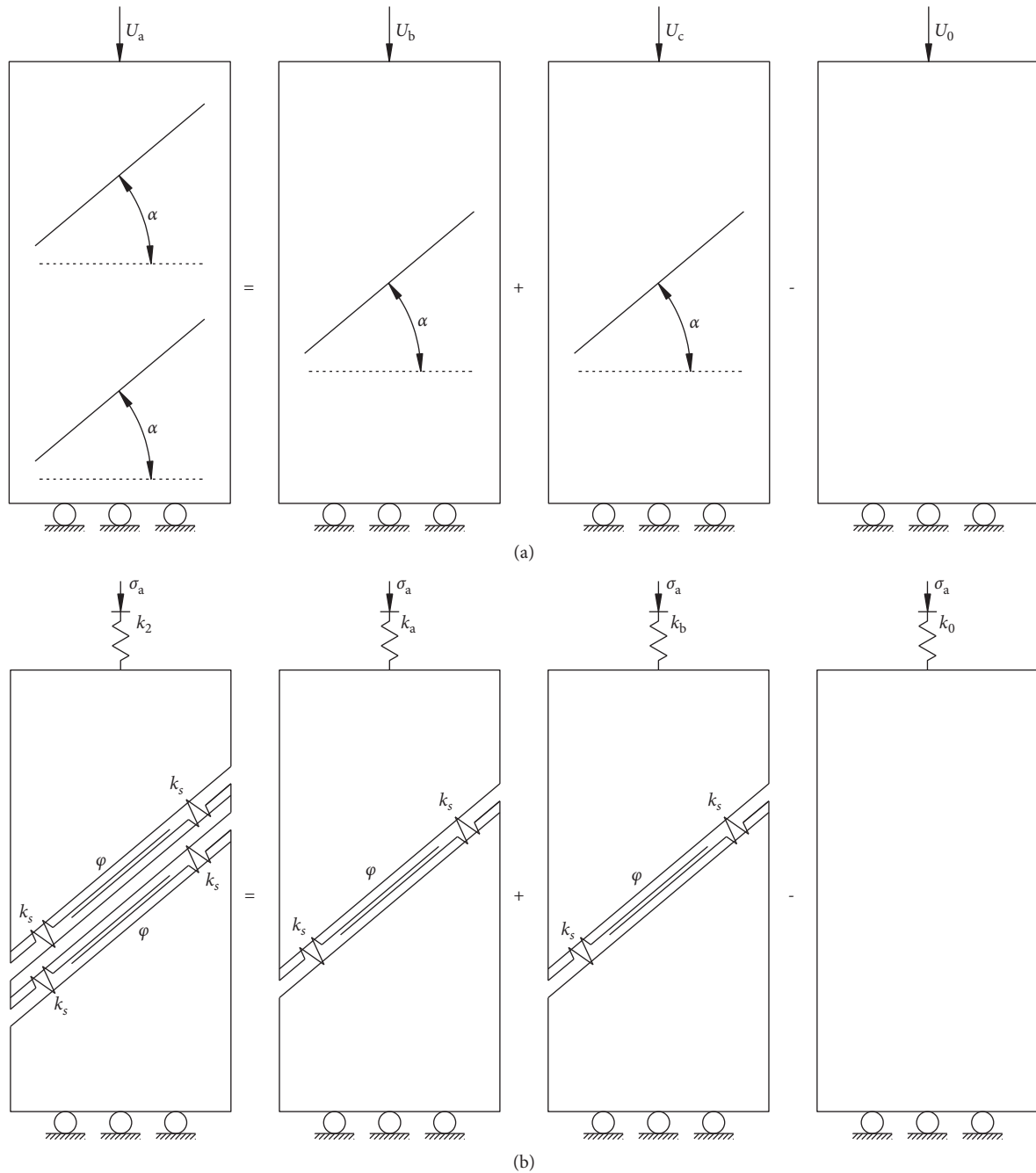
(a)

(b)

FIGURE 5: Model of coal body containing two joints. (a) Combined models for coal containing two joints. (b) The equivalent physical combined models.

of coal with through-going joints gradually increases; the damage variable grows much more when the number of joints is less than 20 while varies less when there are more than 20 joints (Figure 7).

In a case where two, three, five, ten, and twenty through-going joints are present in coal containing joints, the damage variables at different dip angles of joints are all larger than 0.5, 0.6, 0.7, 0.8, and 0.9, respectively; when the number of joints tends to be infinite, the damage variables all approached to 1. On this condition, the coal with joints is completely damaged (Table 1), which implies that the number of joints plays a decisive role in damage to the coal. Given fixed dimensions of coal with joints, the joint spacing (d) is inversely proportional to the number of joints. Thus, the lower the joint spacing, the larger the damage variable of coal containing joints.

Above all, the relationships of the damage variable D of coal containing through-going joints with the dip angle α, azimuth β, and spacing d (number n) of joints are expressed as follows:
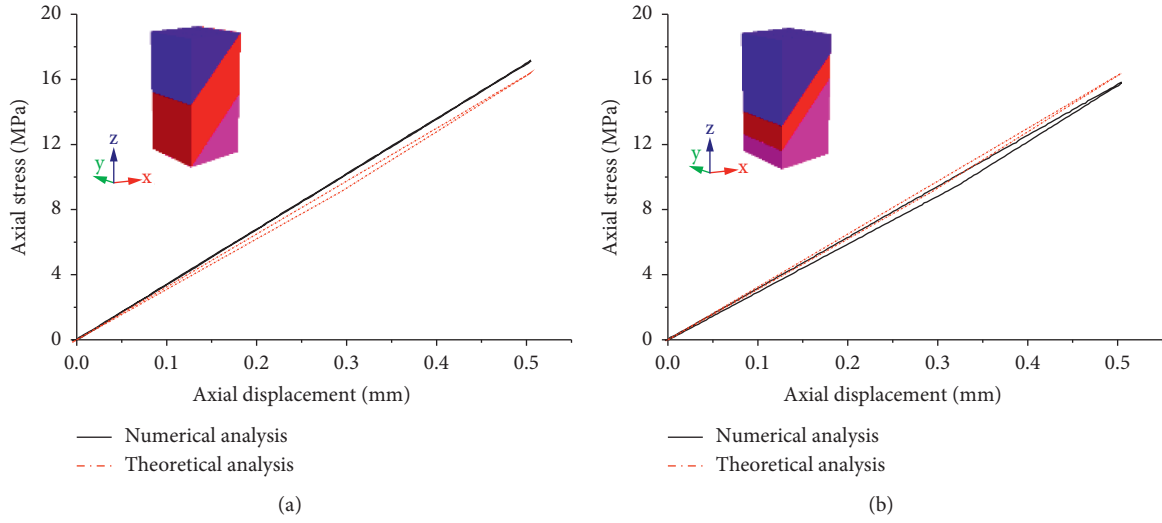
(a)

(b)

FIGURE 6: Comparison of numerical and theoretical results of coal body containing two joints. (a) When two joints are located at two ends of the model. (b) When two joints are situated in the middle of the model.
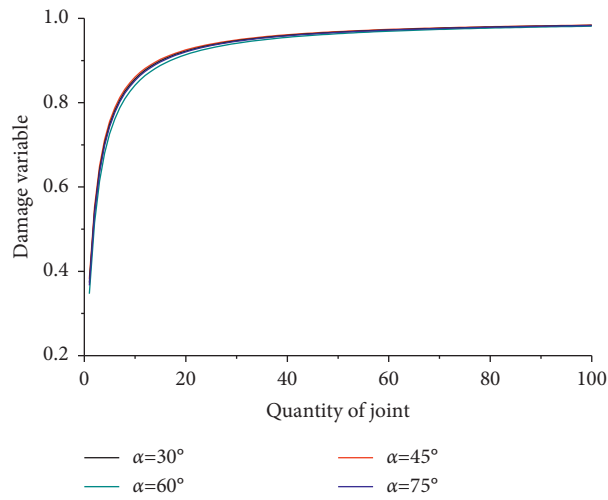

FIGURE 7: The change in the damage variable of coal with the number of joints.

TABLE 1: The influence of the number of joints on the damage variable of coal containing through-going joints.

Number of through-going joints	Dip angle of joints (°)			
	30	45	60	75
1	0.37	0.38	0.35	0.37
2	0.54	0.55	0.52	0.54
3	0.64	0.65	0.61	0.63
4	0.70	0.71	0.68	0.70
5	0.75	0.76	0.73	0.74
⋮	⋮	⋮	⋮	⋮
10	0.86	0.86	0.84	0.85
⋮	⋮	⋮	⋮	⋮
20	0.92	0.93	0.91	0.92
⋮	⋮	⋮	⋮	⋮
100	0.98	0.98	0.98	0.98

$$D = \begin{cases} \dfrac{nEWK_n\sin^2 \alpha \cos \alpha \cos \beta + nEWK_s\cos^3 \alpha \cos \beta}{B_bHK_nK_s + nEWK_n\sin^2 \alpha \cos \alpha \cos \beta + nEWK_s\cos^3 \alpha \cos \beta}, & \beta \leq \arctan\dfrac{W}{B_b}, \alpha \leq \arctan\dfrac{H}{W}, \\[2em] \dfrac{nEK_n\sin^2 \alpha \cos \alpha \sin \beta + nEK_s\cos^3 \alpha \sin \beta}{HK_nK_s + nEK_n\sin^2 \alpha \cos \alpha \sin \beta + nEK_s\cos^3 \alpha \sin \beta}, & \beta > \arctan\dfrac{W}{B_b}, \alpha \leq \arctan\dfrac{H}{W}, \\[2em] \dfrac{nEWK_n\sin^3 \alpha + nEWK_s\cos^2 \alpha \sin \alpha}{H^2K_nK_s + nEWK_n\sin^3 \alpha + nEWK_s\cos^2 \alpha \sin \alpha}, & \alpha > \arctan\dfrac{H}{W}. \end{cases} \tag{12}$$

When $H = 6$ m and $W = B_b = 1s$ m, the curves attained by using 3DEC numerical simulation software remain similar to those obtained through theoretical analysis (Equation (12)), as shown in Figure 8. It reveals that it is feasible to analyse the influence of the orientation of joints on the support capacity of coal walls in a large-mining-height working face based on Equation (12).

3. The Influence of Joints on the Distribution of Abutment Pressure on a Large-Mining-Height Working Face

According to a previous study [10], the abutment pressure σy at a position x away from the coal walls within the LEZ in front of the working face is calculated as follows:

$$\sigma_y = N_0 e^{2fx/M(1+\sin \varphi/1-\sin \varphi)}, \tag{13}$$

where N_0, f, φ, and M denote the support capacity of coal walls, friction coefficient between strata, internal friction angle of coal, and the mining height of the working face, respectively.

According to Equation (13), it is found that the abutment pressure at $x = 0$ denotes the support capacity of coal walls. The abutment pressure within the LEZ is influenced by various factors such as the support capacity of coal walls, mining height, the friction coefficient between strata, and the internal friction angle of the coal.

The critical pressure (support capacity) on coal walls can be calculated according to the theory of the stability of columns [26–28].

$$\sigma_0 = \frac{\pi^2 E_{em} I}{4M^2 S}, \tag{14}$$

$$E_{em} = (1 - D)E_m, \tag{15}$$

where E_{em}, E_m, and D represent the elastic modulus of coal after mining-induced damage, the elastic modulus of intact coal, and the damage variable, respectively [29]; I refers to the moment of inertia of the neutral axis of a section and $I = \pi dc4/64$ as for a

circular section, in which dc denotes the diameter of the section; S denotes the cross-sectional area of the column, with $S = \pi dc2/4$. According to Equation (14), it can be obtained that the support capacity N_0 of the coal walls is related not only to the mining height but also to the elastic modulus of the coal.

When the diameter of the cross section of the column for coal walls is the unit length, the support capacity of coal walls presents an analogous hyperbolic relationship with the mining height if the elastic modulus of damaged coal is taken as 0.5 GPa (Figure 9(a)); by setting the mining height to 6 m, the support capacity of coal walls is linearly correlated with the elastic modulus of damaged coal (Figure 9(b)); the result obtained through numerical simulation also verifies the relationships of the support capacity of coal walls with the mining height and elastic modulus of coal (Figure 10).

Based on Equations (13) and (14), the abutment pressure σ_y at a position x away from the coal walls within the LEZ in a large-mining-height working face based on the theory on stability of columns of coal walls can be attained:

$$\sigma_y = \frac{\pi^2 E_{em} I}{4M^2 S} e^{2fx/M(1+\sin \varphi/1-\sin \varphi)}. \tag{16}$$

As a result, the abutment pressure at the same position within the LEZ in a large-mining-height working face under given conditions is mainly influenced by mechanical parameters of coal. Therefore, the influence of parameters of joints on the abutment pressure within the LEZ in a large-mining-height working face can be elucidated according to the influence of the joints on the damage to the coal.

3.1. Theoretical Analysis on the Influence of the Orientation of Joints

3.1.1. The Influence of the Dip Angle of the Joints. According to Equations (5) and (16) and assuming $H = M$, the relationship between the abutment pressure σ_y at a position x away from the coal walls within the LEZ in a large-mining-height working face and the dip angle of joints can be expressed as follows:
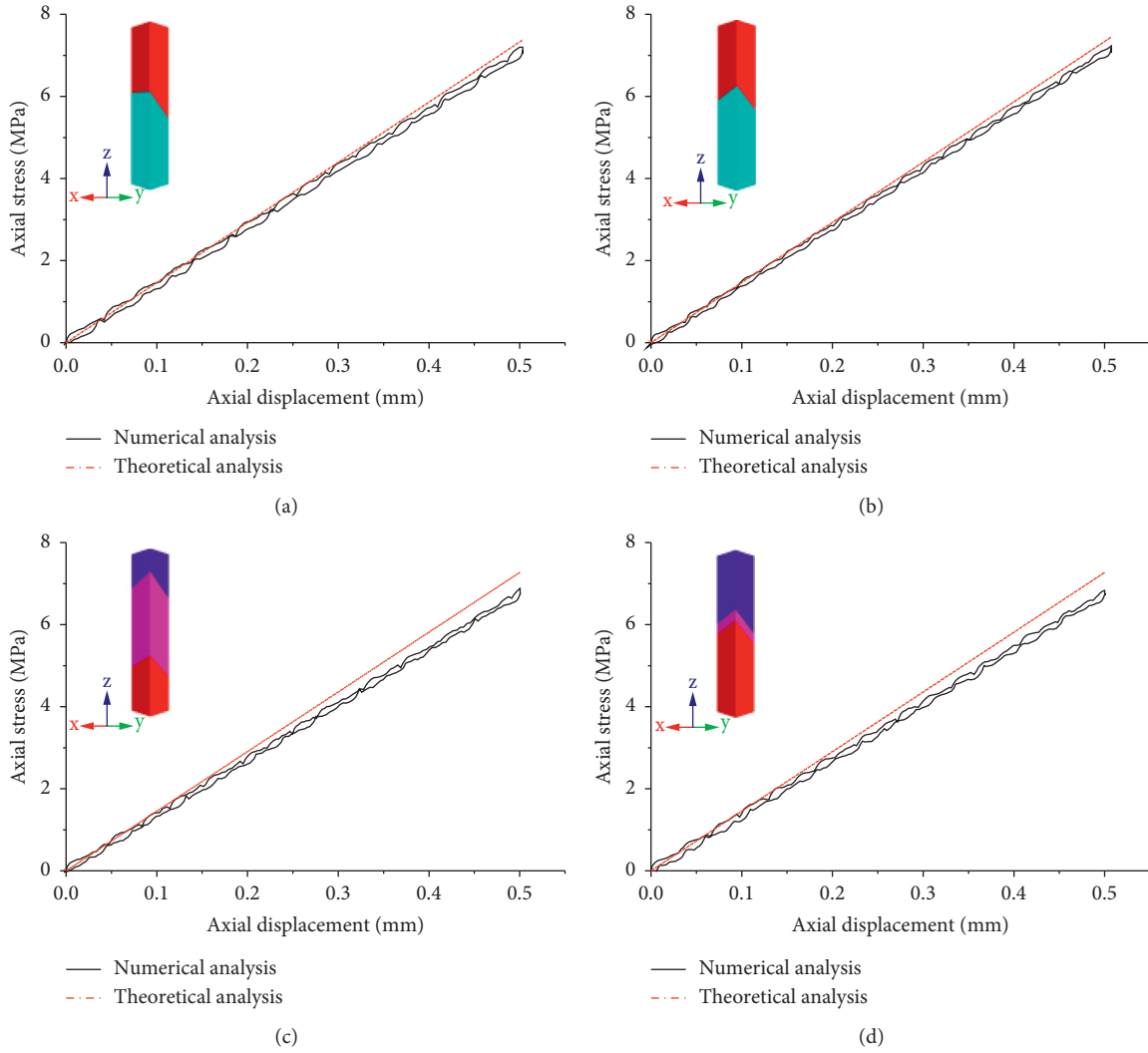
FIGURE 8: Comparison of numerical and theoretical results under different conditions with the coal with joints at $H = 6$ m. (a) $\alpha = 45°$, $\beta = 0°$ and $n = 1$. (b) $\alpha = 45°$, $\beta = 45°$ and $n = 1$. (c) $\alpha = 45°$, $\beta = 45°$ and $n = 2$ (joints located at two ends of the model). (d) $\alpha = 45°$, $\beta = 45°$ and $n = 2$ (joints located in the middle of the model).
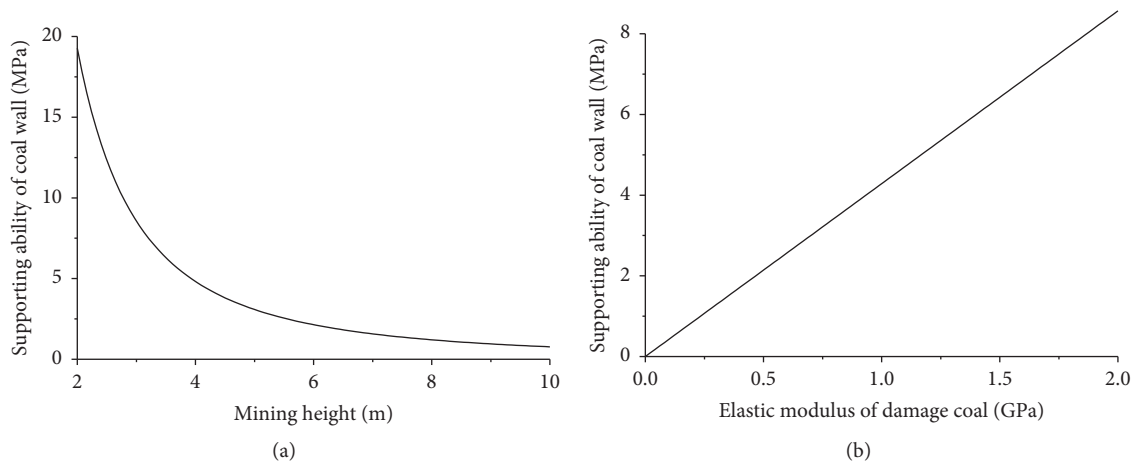

FIGURE 9: Influence factors of coal wall supporting ability. (a) The influence of the mining height ($E_{em} = 0.5$ GPa). (b) The influence of the elastic modulus of coal ($M = 6.0$ m).
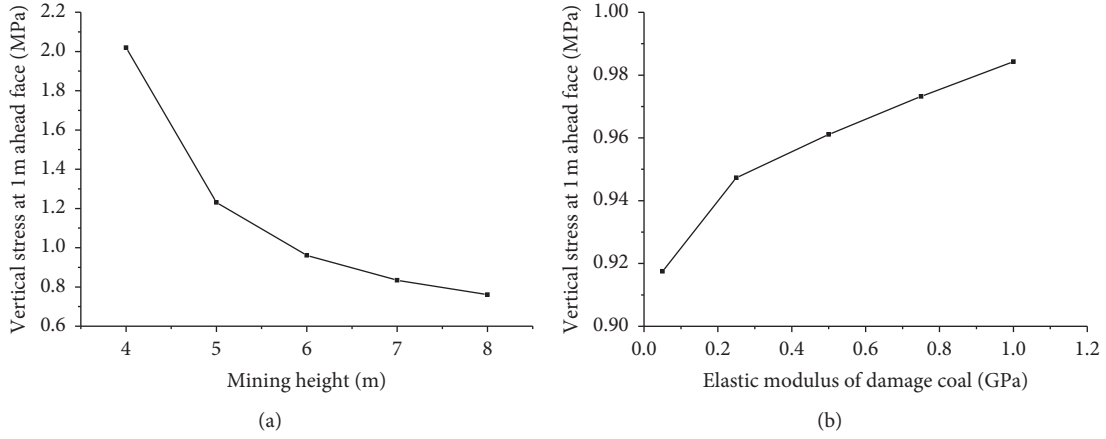
(a)

(b)

FIGURE 10: Vertical stress on working face. (a) The influence of the mining height ($E_{em} = 0.5$ GPa). (b) The influence of the elastic modulus of coal ($M = 6.0$ m).

$$\sigma_y = \begin{cases} \dfrac{\pi^2 E_m I K_n K_s}{4MS\left(MK_nK_s + EK_n\sin^2 \alpha \cos \alpha + EK_s\cos^3 \alpha\right)}e^{e^{2fx/M(1+\sin \varphi/1-\sin \varphi)}}, & \alpha \leq \arctan\dfrac{M}{W}, \\[4mm] \dfrac{\pi^2 E_m I K_n K_s}{4S\left(M^2K_nK_s + EWK_n\sin^3 \alpha + EWK_s\cos^2 \alpha \sin \alpha\right)}e^{e^{2fx/M(1+\sin \varphi/1-\sin \varphi)}}, & \alpha > \arctan\dfrac{M}{W}. \end{cases} \tag{17}$$

As shown in Equation (17), the change in abutment pressure at $x = 0.5$ m within the LEZ in a large-mining-height working face with the dip angle of joints is obtained under the mining height of the working face of $M = 6$ m, $W = B_b = 1$ m, $E_m = 10$ GPa, $K_n = 10$ GPa/m, and $K_s = 4$ GPa/ m, as shown in Figure 11.

As shown in Figure 11, the abutment pressure within the LEZ in a large-mining-height working face first decreases, then rises, and finally increases when increasing the dip angle of the joints in coal seams: this influence is opposite to that of the dip angle of joints on the damage to intact coal; the abutment pressure varies between 6.39 and 7.45 MPa. The result indicates that the change of the dip angle of joints

in coal seams affects the abutment pressure within the LEZ in the large-mining-height working face to some extent.

3.1.2. The Influence of the Azimuth of the Joints. According to the above analysis, the azimuth of joints in coal seams does not influence the damage to the coal when $\alpha > \arctan (H/W)$; according to Equations (7) and (16) and assuming $H = M$, the relationship between the abutment pressure σ_y at a position x away from coal walls within the LEZ in a large-mining-height working face and the azimuth of joints is shown in Equation (18) at $\alpha \leq \arctan (H/W)$:

$$\sigma_y = \begin{cases} \dfrac{\pi^2 E_m I B_b K_n K_s}{4MS\left(B_bMK_nK_s + EWK_n\sin^2 \alpha \cos \alpha \cos \beta + EWK_s\cos^3 \alpha \cos \beta\right)}e^{e^{2fx/M(1+\sin \varphi/1-\sin \varphi)}}, & \beta \leq \arctan\dfrac{W}{B_b}, \\[4mm] \dfrac{\pi^2 E_m I K_n K_s}{4MS\left(MK_nK_s + EK_n\sin^2 \alpha \cos \alpha \sin \beta + EK_s\cos^3 \alpha \sin \beta\right)}e^{e^{2fx/M(1+\sin \varphi/1-\sin \varphi)}}, & \beta > \arctan\dfrac{W}{B_b}. \end{cases} \tag{18}$$

As shown in Equation (18), the change in the abutment pressure at $x = 0.5$ m within the LEZ in a large-mining-height working face with the dip angle of joints is attained under the mining height of the working face of $M = 6$ m, $W = B_b = 1$ m, $E_m = 10$ GPa, $K_n = 10$ GPa/m, and $K_s = 4$ GPa/ m, as shown in Figure 12.

It can be seen from Figure 12 that the abutment pressure within the LEZ in a large-mining-height working face first

increases, then decreases with the increasing azimuth at different dip angles of the joints. The maximum abutment pressure is found at the azimuth of $\beta = 45°$ (Figure 12). At dip angles of the joints of $30°$, $45°$, and $60°$, the abutment pressures vary in the ranges of 6.43 to 6.76, 6.39 to 6.73, and 6.55 to 6.85 MPa: this indicates that the azimuth of through-going joints in coal seams shows a certain (albeit slight) influence on the abutment pressure within the LEZ.
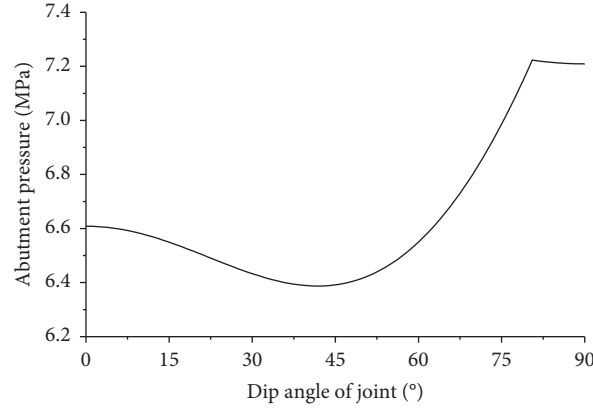
FIGURE 11: Change in abutment pressure in LEZ with inclination angle of joints in a fully mechanised working face with a large mining height.
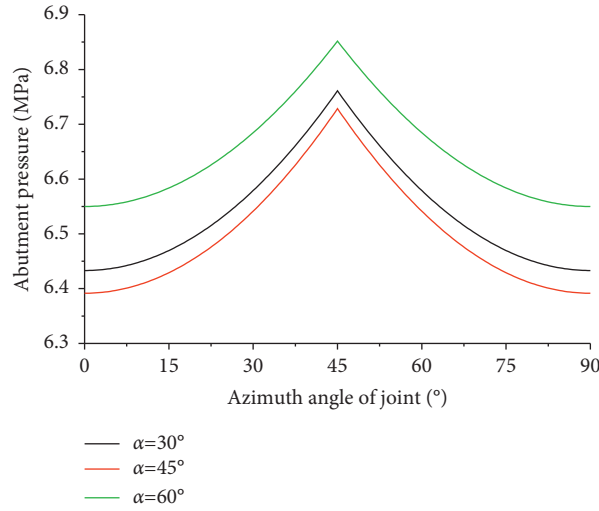

FIGURE 12: Change in the abutment pressure in LEZ with azimuth angle of joints in a fully mechanised working face with large mining height.

3.1.3. Joint Spacing. Based on the above analysis, the joint spacing in coal seams is inversely proportional to the number of joints within a certain range. Thus, it is feasible to obtain the influence of the joint spacing by analysing the influence of the number of joints on the abutment pressure within the LEZ in a large-mining-height working face.

According to Equations (11) and (16), and assuming $H = M$, the relationship between the abutment pressure σ_y at a position x away from coal walls within the LEZ in a large-mining-height working face and the number of joints can be attained:

$$
\sigma_y = \begin{cases} \dfrac{\pi^2 E_m I K_n K_s}{4MS\left(MK_n K_s + nEK_n \sin^2 \alpha \cos \alpha + nEK_s \cos^3 \alpha\right)} e^{e^{2fx/M(1+\sin \varphi/1-\sin \varphi)}}, & \alpha \le \arctan \dfrac{M}{W}, \\[4mm] \dfrac{K_n K_s}{4S\left(M^2 K_n K_s + nEWK_n \sin^3 \alpha + nEWK_s \cos^2 \alpha \sin \alpha\right)} e^{e^{2fx/M(1+\sin \varphi/1-\sin \varphi)}}, & \alpha > \arctan \dfrac{M}{W}. \end{cases}
\tag{19}
$$

As shown in Equation (19), under the mining height of the working face $M = 6$ m, $W = B_b = 1$ m, $E_m = 10$ GPa, $K_n = 10$ GPa/m, and $K_s = 4$ GPa/m, the change law of the abutment pressure at the position of $x = 0.5$ m within the LEZ in a large-mining-height working face with the dip angle of joints is shown in Figure 13.
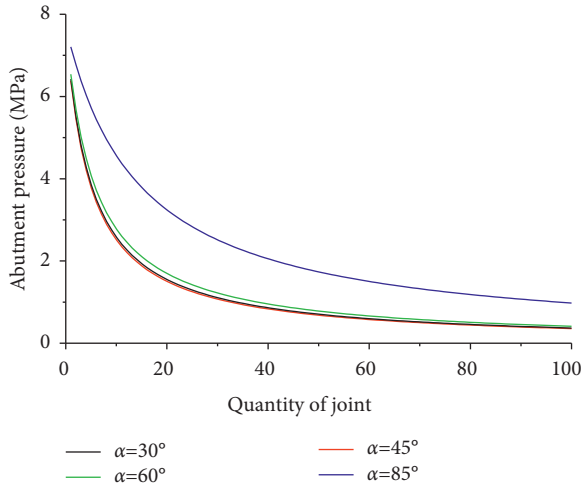
FIGURE 13: Change in abutment pressure in LEZ with number of joints in a fully mechanised working face with large mining height.

As shown in Figure 13, the abutment pressures within the LEZ in a large-mining-height working face all gradually decrease with an increase in the number of joints at different dip angles. The advanced abutment pressure within the LEZ decreases significantly when there are fewer than 20 joints, while it does so much less when the number of joints is greater than 20. By taking the dip angle of the joints as $\alpha = 45°$ as an example, the abutment pressure at $x = 0.5$ m within the LEZ is about 7.71 MPa for coal seams without joints while it is about 1.50 MPa in the case that 20 joints are present in the coal seams. This indicates that the number of joints in coal seams significantly influences the abutment pressure within the LEZ in a large-mining-height working face. The result suggests that the joint spacing in coal seams delivers a great influence on the abutment pressure within the LEZ; moreover, with the reduction of joint spacing, the abutment pressure at the same distance from the working face within the LEZ gradually decreases.

3.2. Numerical Simulation Analysis of the Influence of Joint Orientation.
To verify the rationality of the theoretical analysis, the influence of the orientation of the joints on the abutment pressure of the LEZ in a large-mining-height working face during the mining of coal seams was simulated and analysed by using 3DEC numerical simulation software.

The 4309 working face was used as the numerical engineering background. The 4309 working face belongs to the Sihe Coal Mine, located in Jincheng, Shanxi province, Central China. The thickness of the coal seam is 6.14 m and the immediate roof is sandy mudstone, 12.58 m, as shown in Figure 14.

To ensure the rationality and operability of the numerical simulation, a total of nine numerical models were established according to the field measurements [30–32] and research objective, as shown in Table 2 and Figure 15.

3.2.1. The Dip Angle of Joints.
Figure 16 shows the changes in abutment pressures at the same position within the LEZ in

the large-mining-height working face under different dip angles of joints: the advanced abutment pressures within the LEZ in the large-mining-height working face vary under the effect of the dip angle of joints; at joint dip angles of 45° and 135°, the abutment pressures at the same position within the LEZ are similar while they are both lower than that at 90°. This conforms to the result obtained through theoretical analysis, which indicates the rationality thereof.

3.2.2. The Azimuth of the Joints.
Figure 17 displays the changes in abutment pressures at the same position within the LEZ in the large-mining-height working face under different joint azimuths: the advanced abutment pressures within the LEZ in the large-mining-height working face differ due to the influence of the azimuth of joints; when the azimuths of joints are separately 45° and 135°, the abutment pressures at the same position within the LEZ are quasi-equivalent while they are both larger than that at the azimuth of 0°. This matches the result attained through theoretical analysis, which reveals the rationality thereof.

3.2.3. The Joint Spacing.
Figure 18 shows the changes in abutment pressures at the same position within the LEZ in the large-mining-height working face with different joint spacings in the coal seams: under the influence of the spacings of through-going joints in coal seams, the advanced abutment pressures at the same position within the LEZ in the large-mining-height working face are different; the highest and lowest abutment pressures are present in the LEZ under the corresponding joint spacings of 5 and 1.41 m, respectively; this is consistent with the result acquired through theoretical analysis, indicative of the rationality of the theoretical analysis.

With the excavation of the working face, the abutment pressures within the LEZ in the large-mining-height working face under different orientations of joints all present the same periodic fluctuation under the influence of periodic weighting of the roof. This suggests that the orientation of joints in coal seams influences the abutment pressure within the LEZ only by affecting the support capacity of the large-mining-height coal walls. It does not affect the spatiotemporal change in the advanced abutment pressure in the large-mining-height working face with the advance of the working face.

Overall, the influence of the orientation of joints in coal seams on the abutment pressure within the LEZ in the large-mining-height working face is summarised as follows: with increasing dip angle of the joints, the abutment pressure at the same position within the LEZ first decreases, then increases, and finally decreases; under certain conditions, the abutment pressure at the same position within the LEZ first increases, then decreases with the increasing azimuth of the joints; as the joint spacing increases, the number of joints gradually decreases and correspondingly the abutment pressure at the same position within the LEZ rises; however, the dip angle and azimuth of joints only marginally influence the abutment pressure within the LEZ. In addition, the orientation of through-going joints in coal seams only affects
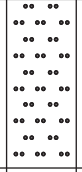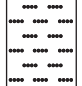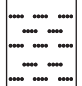
Cumulative Thickness (m)	Strata Thickness (m)	Stratigraphic Column	Lithology Description
318.50	18.50		Fine sandstone
321.00	2.50		Siltstone
34.90	13.90		Sandy mudstone
338.90	4.00		Siltstone
351.48	12.58		Sandy mudstone
357.62	6.14		3#coal
363.76	13.18		Sandy mudstone

FIGURE 14: Comprehensive Column of 4309 working face.

TABLE 2: Occurrence of joints with different parameters in coal seam.

Serial number	Properties of joints	Parameters of joints			Remarks
		Dip angle α (°)	Azimuth β (°)	Spacing d (m)	
1		45			A model
2		90	0		B Model
3	Primary joint	135		5	C Model
4		45	45		D model
5			135		E model
6	Primary joint	90		2	F Model
	Secondary joint	45			
7	Primary joint	90		2	G model
	Secondary joint	45	0	1.41	
8	Primary joint	90		2	H Model
	Secondary joint	135			
9	Primary joint	90		2	I Model
	Secondary joint	135		1.41	

Note: The dip angle α of joints refers to the included angle between the dip direction of joints and the Y-axis positive direction (advancing direction) in 3DEC software; the azimuth β denotes the included angle between the strike direction of joints and X-axis positive direction (the direction along the length of the working face).

the abutment pressure within the LEZ while it shows no influence on the spatiotemporal change in the advanced abutment pressure in the large-mining-height working face with the advance of the working face.

Above all, the relationship between the orientation of joints in coal seams and the abutment pressure within the LEZ in the large-mining-height working face is described as follows:
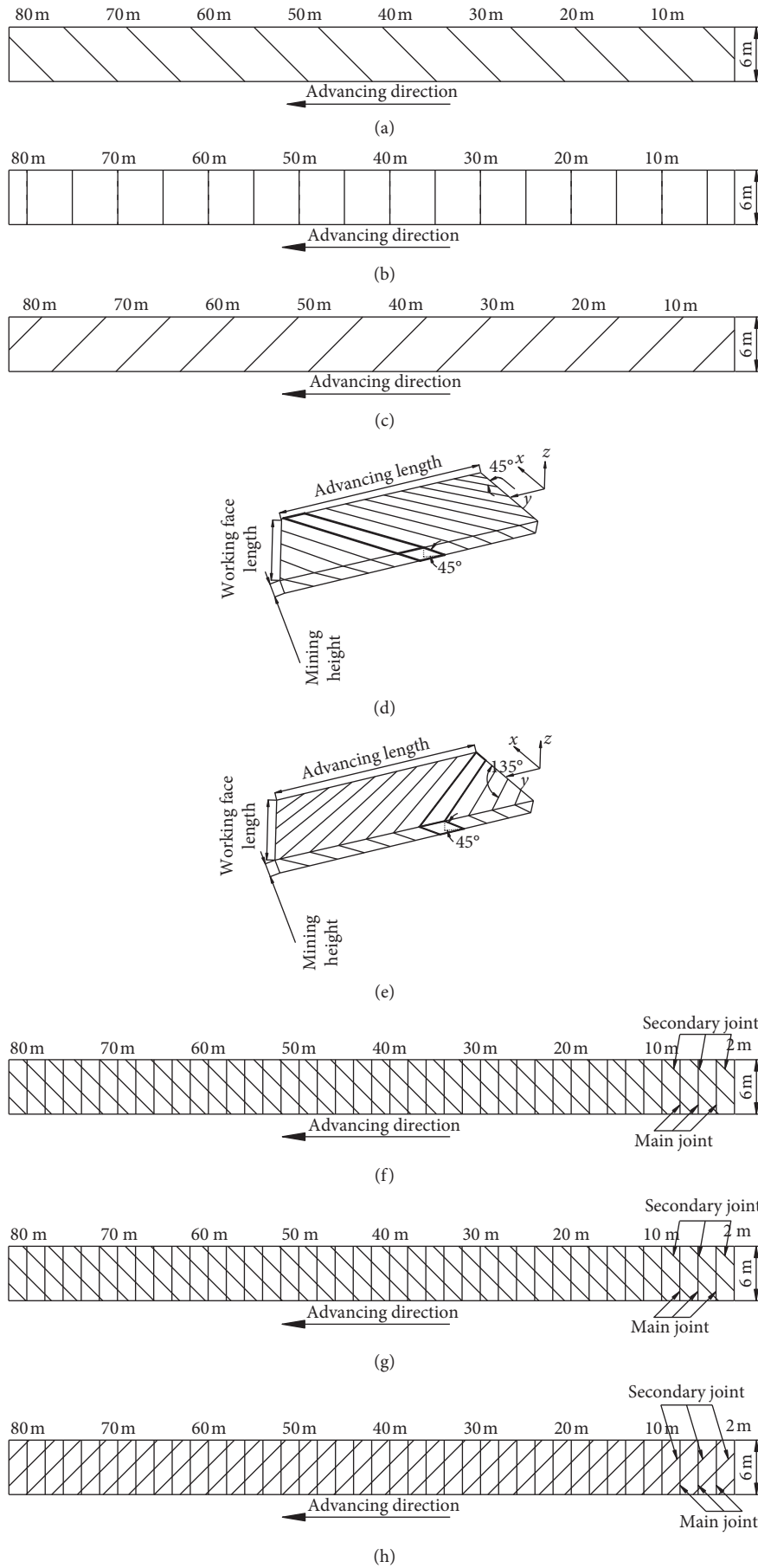
(a)

(b)

(c)

(d)

(e)
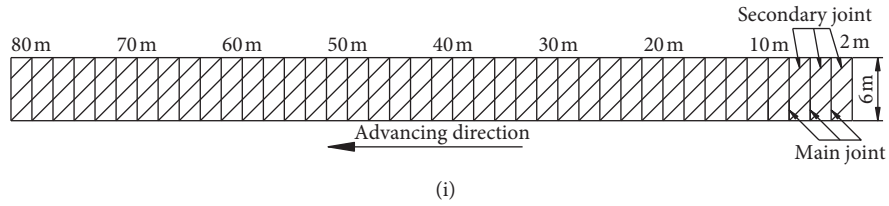
(f)

(g)

(h)

Figure 15: Continued.

(i)

FIGURE 15: Model section of joints with different parameters in a coal seam. (a) Model A. (b) Model B. (c) Model C. (d) Model D. (e) Model E. (f) Model F. (g) Model G. (h) Model H. (i) Model I.
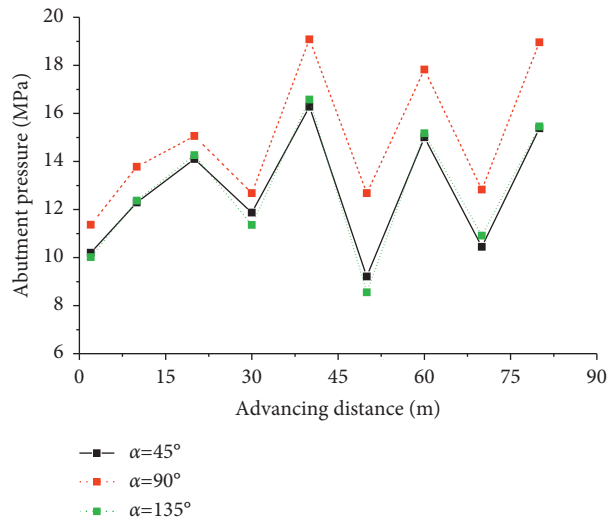

FIGURE 16: Abutment pressure distribution in the limit equilibrium area with different joint inclination angles.
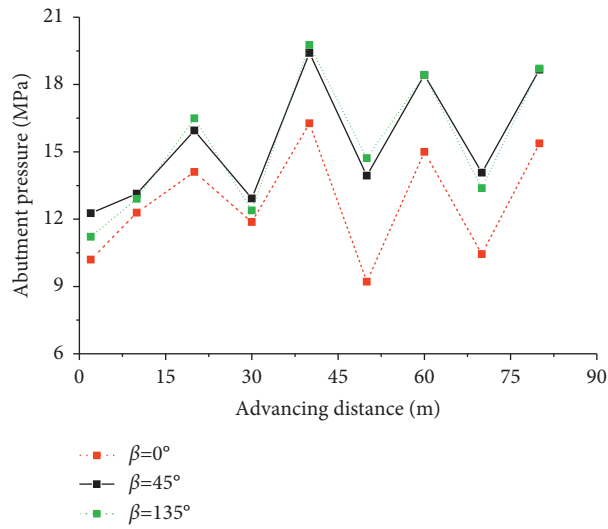

FIGURE 17: Abutment pressure distribution in the limit equilibrium area with different joint azimuth angles.
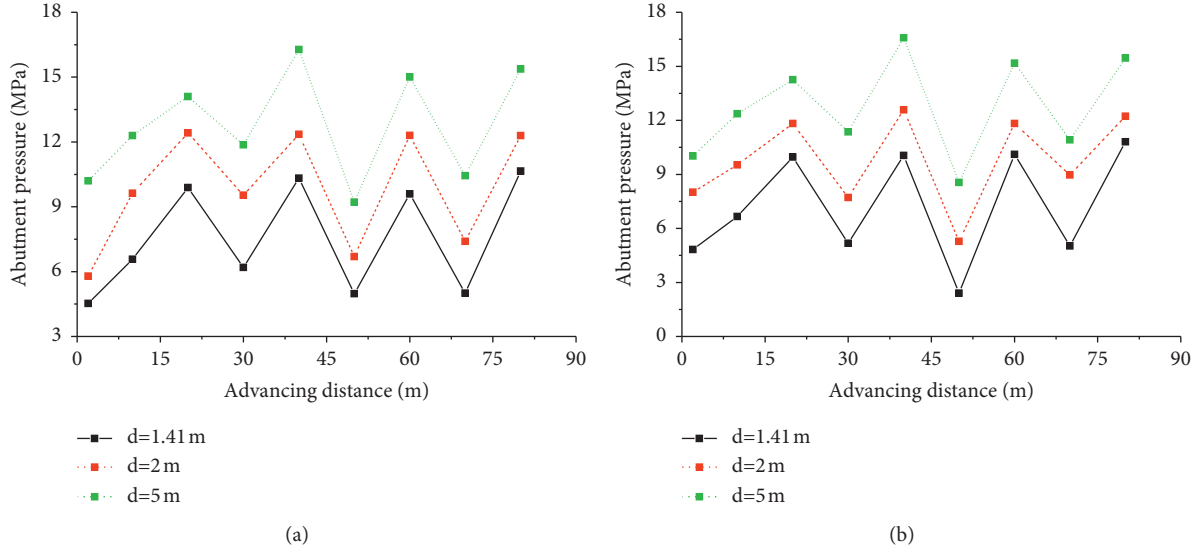
FIGURE 18: Abutment pressure distribution in the limit equilibrium area with different joint spacings. (a) Dip angle of joint of 45°. (b) Dip angle of joint of 135°.

$$\sigma_y = \begin{cases} \dfrac{\pi^2 E_m IBK_n K_s}{4MS\left(BMK_n K_s + nEWK_n\sin^2\alpha\,\cos\alpha\,\cos\beta + nEWK_s\cos^3\alpha\,\cos\beta\right)} e^{e^{2fx/M(1+\sin\varphi/1-\sin\varphi)}}, & \beta \le \arctan\dfrac{W}{B}, \alpha \le \arctan\dfrac{M}{W}, \\[4mm] \dfrac{\pi^2 E_m IK_n K_s}{4MS\left(MK_n K_s + nEK_n\sin^2\alpha\,\cos\alpha\,\sin\beta + nEK_s\cos^3\alpha\,\sin\beta\right)} e^{e^{2fx/M(1+\sin\varphi/1-\sin\varphi)}}, & \beta > \arctan\dfrac{W}{B}, \alpha \le \arctan\dfrac{M}{W}, \\[4mm] \dfrac{\pi^2 E_m IK_n K_s}{4S\left(M^2 K_n K_s + nEWK_n\sin^3\alpha + nEWK_s\cos^2\alpha\,\sin\alpha\right)} e^{e^{2fx/M(1+\sin\varphi/1-\sin\varphi)}}, & \alpha > \arctan\dfrac{M}{W}. \end{cases} \tag{20}$$

4. Conclusion

(1) The damage variable of coal with joints first increases, then decreases, and finally increases with increasing dip angle of the joints; an increase in the azimuth of joints corresponds to the first decrease and then growth in the damage variable of coal with joints; the damage variable of coal with joints gradually decreases as the joint spacing is increased.

(2) Based on the theory on the stability of columns of coal walls in the large-mining-height working face, the distribution and the main influencing factors of the abutment pressure within the LEZ were investigated. As for a large-mining-height working face in the given conditions, the abutment pressure at the same position within the LEZ is mainly affected by mechanical parameters of the coal.

(3) With increasing joint dip angle, the abutment pressure at the same position in front of coal walls first decreases, then increases, only to decrease again; under certain conditions, the abutment pressure at the same position within the LEZ first increases, then

decreases as the azimuth of the joints increases; an increase in the joint spacing corresponds to the growth of the abutment pressure at the same position within the LEZ. The dip angle and azimuth of the joints exert an insignificant influence on the abutment pressure within the LEZ.

Data Availability

All the data and models generated or used during the study appear in the submitted article.

Conflicts of Interest

The authors declare that there are no conflicts of interest regarding the publication of this paper.

Acknowledgments

References

[1] G.-F. Wang, Y. -H. Pang, M.-Z. Li, Y. Ma, and X. -H. Liu, "Hydraulic support and coal wall coupling relationship in ultra large height mining face," *Journal of China Coal Society*, vol. 42, pp. 518–526, 2017.

[2] Y.-X. Xu, G.-F. Wang, M. Z. Li, Y.-J. Xu, H.-J. Han, and J.-H. Zhang, "Investigation on coal face slabbed spalling features and reasonable control at the longwall face with super large cutting height and longwall top coal caving method," *Journal of China Coal Society*, vol. 46, pp. 357–369, 2020.

[3] J.-C. Wang, Z.-H. Wang, and D.-Z. Kong, "Failure and prevention mechanism of coal wall in hard coal seam," *Journal of China Coal Society*, vol. 40, pp. 2243–2250, 2015.

[4] H.-W. Zhang, K.-Y. Zhou, X. Fu, and F. Zhu, "Strata behaviour characteristics of super high mining height working face," *Journal of Liaoning Technical University*, vol. 37, pp. 1–6, 2018.

[5] B.-J. Fu, M. Tu, and M.-Z. Gao, "Study on unloading instability model of working face with large mining height," *Journal of Mining & Safety Engineering*, vol. 34, pp. 1128–1133, 2017.

[6] D.-Z. Kong, Y. Liu, and Q.-Z. Liu, "Study of coal face failure mechanism of a large-cutting-height mining face," *Chinese Journal of Rock Mechanics and Engineering*, vol. 37, pp. 3458–3469, 2018.

[7] S.-F. Yin, F.-L. He, Y.-H. Wang, J.-J. Shi, Z.-H. Cheng, and L.-L. Sui, "An experimental study of layered weakening mechanism to nonsynchronous spalling from composite rib with large mining height," *JOurnal of China University of Mining & Technology*, vol. 48, pp. 750–759, 2019.

[8] G.-F. Song, S.-L. Yang, and Z.-H. Wang, "Longwall face stability analysis using Ｒitz method and its 3D physical modelling study," *Journal of China Coal Society*, vol. 43, pp. 2162–2172, 2018.

[9] K. Yang, S. Liu, C.-A. Tang, Z. Wei, and X.-L. Chi, "Mechanism and prevention of coal seam rib spalling in remote protected layer across coal group," *Journal of China Coal Society*, vol. 44, pp. 2611–2621, 2019.

[10] Z.-S. Meng, Q.-L. Zeng, K.-D. Gao, S. Kong, P. Liu, and L.-R. Wang, "Failure analysis of super-large mining height powered support," *Engineering Failure Analysis*, vol. 92, pp. 378–391, 2018.

[11] G.-A. Zhu, L.-M. Dou, C.-B. Wang, J. Li, and W. Cai, "Numerical investigation of the evolution of overlying strata and distribution of static and dynamic loads in a deep island coal panel," *Arabian Journal of Geosciences*, vol. 10, p. 549, 2017.

[12] S. Prusek, M. Plonka, and A. Walentek, "Applying the ground reaction curve concept to the assessment of shield support performance in longwall faces," *Arabian Journal of Geosciences*, vol. 9, p. 167, 2016.

[13] S.-S. Peng, *Coal Mine Ground Control*, Society for Mining Metallurgy, Chicago, IL, US, 3rd edition, 2008.

[14] J.-F. Ju and J. L. Xu, "Structural characteristics of key strata and strata behaviour of a fully mechanized longwall face with 7.0 m height chocks," *International Journal of Rock Mechanics and Mining Sciences*, vol. 58, pp. 46–54, 2013.

[15] W.-B. Guo, C.-Y. Liu, G.-W. Dong, and W.-Y. Lv, "Analytical study to estimate rib spalling extent and support requirements in thick seam mining," *Arabian Journal of Geosciences*, vol. 12, no. 8, p. 276, 2019.

[16] M.-G. Qian, J.-L. Xu, J.-C. Wang, and Y.-P. Wu, *Ground Pressure and Strata Control*, China University of Mining & Technology Press, Xuzhou, China, 3rd edition, 2020.

[17] Y. Ning, "Mechanism and control technique of the rib spalling in fully mechanized mining face with great mining height," *Journal of China Coal Society*, vol. 34, pp. 50–52, 2009.

[18] Q.-X. Huang and J.-H. Liu, "Vertical slice model for coal wall spalling of large mining height longwall face in shallow seam," *Journal of Mining & Safety Engineering*, vol. 32, pp. 187–191, 2015.

[19] J.-X. Yang, C.-Y. Liu, F.-F. Wu, and Y. Yang, "The research on the coal wall stability mechanism in larger height coal seam with a stratum of gangue," *Journal of Mining & Safety Engineering*, vol. 30, pp. 856–862, 2013.

[20] W.-A. Olsson, "Experiments on a slipping crack," *Geophysical Research Letters*, vol. 9, pp. 797–800, 1982.

[21] B. H. G. Brady, M. L. Cramer, and R. D. Hart, "Preliminary analysis of a loading test on a large basalt block," *International Journal of Rock Mechanics and Mining Science & Geomechanics Abstracts*, vol. 22, pp. 345–348, 1985.

[22] C. Gerrard, "Equivalent elastic moduli of a rock mass consisting of orthorhombic layers," *International Journal of Rock Mechanics and Mining Science & Geomechanics Abstracts*, vol. 19, pp. 9–14, 1982.

[23] Z.-Y. Zhou, P. Cao, and H. Lin, "The mechanical parameters selection of jointed rock mass in the 3DEC," *West-China Exploration Engineering*, vol. 123, pp. 163–165, 2006.

[24] F. Beer, E. Johnston, J. Dewolf, and D. Mazurek, *Mechanics of Materials*, McGraw-Hill, New York, NY, USA, 6th edition, 2012.

[25] P. Kulatilake, Q. Wu, Z.-X. Yu, and F.-X. Jiang, "Investigation of stability of a tunnel in a deep coal mine in China," *International Journal of Mining Science and Technology*, vol. 23, pp. 579–589, 2013.

[26] X.-F. Li, H.-B. Li, K. Liu et al., "Dynamic properties and fracture characteristics of rocks subject to impact loading," *Chinese Journal of Rock Mechanics and Engineering*, vol. 36, pp. 2393–2405, 2017.

[27] Y.-H. Pang, G.-F. Wang, and H.-W. Ren, "Multiple influence factor sensitivity analysis on coal wall spalling of workface with large mining height," *Journal of Mining & Safety Engineering*, vol. 36, pp. 736–745, 2019.

[28] Z.-H. Wang, J.-C. Wang, Y. Yang, Y.-S. Tang, and L. Wang, "Mechanical relation between support stiffness and longwall face stability within fully-mechanized mining faces," *Journal of China University of Mining & Technology*, vol. 48, pp. 258–267, 2019.

[29] H.-P. Xie, Y. Ju, and Y.-L. Dong, "Discussion of elastic modulus in classical damage definition," *Mechanics in engineering*, vol. 19, pp. 1–5, 1997.

[30] H.-P. Xie, Z.-H. Chen, and J.-C. Wang, "Fractal study on crack distribution in tunnels for sub-level caving mining," *Journal of China Coal Society*, vol. 23, pp. 30–35, 1998.

[31] X.-M. Song, "Correlation between distribution of cracks and fissures in top coal and size of fragment of mining with sublevel caving," *Journal of China Coal Society*, vol. 23, pp. 40–44, 1998.

[32] P.-L. Gong, *Surrounding Rock Control Theory and Application Study of the Coal Face with Greater Mining Height*, Emergency Management Press, Beijing, China, 2006.